LASER STUDIES OF ATMOSPHERIC REACTIONS*

FREDERICK KAUFMAN

Department of Chemistry, University of Pittsburgh, Pittsburgh, PA 15260 (U.S.A.)

Summary

Results from two experimental studies are described: (1) rate studies of HO_x radical–radical reactions with laser-induced fluorescence (LIF) detection of OH and, indirectly, of HO_2 and vacuum UV resonance fluorescence detection of atomic species; (2) quenching and reaction studies of metastable $N_2(A\ ^3\Sigma_u^+)$ using LIF detection in the N_2 first positive system and detection of atomic species by vacuum UV resonance fluorescence. For experiment (1) recent work on the kinetics of the OH + HO_2 reaction is described and compared with other results and with rate theory. For experiment (2), work on the $N_2(A\ ^3\Sigma_u^+)$ + O_2 reaction is summarized, including the kinetics of the reaction for the $v = 0$, $v = 1$ and $v = 2$ states of $N_2(A\ ^3\Sigma_u^+)$, the identity of the product channels and a review of related studies.

1. Introduction

The complex sequence of atmospheric chemical processes arises more or less directly from the primary energy deposition of photons and electrons. In the ensuing excitation, dissociation and ionization steps, excited states and reactive fragments are produced whose further interactions lead to the now reasonably well-known sets of secondary species and their elementary reactions. Laboratory studies of these reactions are heavily dependent on photochemical detection methods such as resonance absorption or fluorescence and laser-induced fluorescence (LIF). Photochemistry thus enters at two levels: in the primary act and in the diagnostics of the subsequent processes. In the present paper we deal principally with the second level. We describe laboratory measurements, using LIF, of the kinetics of ground state radical reactions applicable to the stratosphere, and we also describe quenching and reaction studies of electronically excited molecules applicable to the perturbed thermosphere. The reactant species are OH and HO_2 in the first part and $N_2(A\ ^3\Sigma_u^+)$ in the second. The reactions are studied in cylindrical flow-tube reactors with careful attention to the interplay of kinetics and transport.

* Paper presented at the Xth International Conference on Photochemistry, Iraklion, Crete, Greece, September 6 - 12, 1981.

0047-2670/81/0000-0000/$02.50

2. Experimental details

The apparatus for stratospheric HO_x reaction studies is shown in Fig. 1 and that for $N_2(A)$ processes in Fig. 2. The discharge flow apparatus of Fig. 1 is similar to that used recently for the OH + H_2O_2 reaction [1]. It consists of a Pyrex flow tube of 2.5 cm inside diameter and 110 cm length with a heated or cooled reactor section, 50 cm long, upstream of the LIF and vacuum UV resonance fluorescence detection cell, as earlier described. OH was monitored by LIF at the $P_1(2)$ line of its $^2\Sigma^+ \leftarrow {}^2\pi$, 0–0 band at 308.6 nm, and HO_2 was monitored by rapid conversion to OH with excess NO using the well-known reaction HO_2 + NO → OH + NO_2 [2].

A movable coaxial double injector allowed the generation of HO_2 by the F + H_2O_2 → HF + HO_2 reaction where the fluorine atoms were generated in microwave discharges of CF_4 highly diluted with helium. H_2O_2 was concentrated to 95 - 99 wt.% by slow vacuum distillation and was analyzed by UV absorption near 214 nm as before [1]. Flow tube and injector surfaces were coated with Teflon or Halocarbon wax to give small reproducible wall removal rate constants of about 8 s^{-1} for OH and 2 - 5 s^{-1} for HO_2. The reaction OH + HO_2 → H_2O + O_2 was studied under conditions of excess HO_2 (less than approximately 1.5×10^{12} cm^{-3}) and with OH (initial concentration, less than approximately 4×10^{10} cm^{-3}) produced by the reaction sequence H + F_2 → HF + F and F + H_2O → HF + OH, in order not to introduce NO (by H + NO_2 → OH + NO) which would regenerate OH by reaction with HO_2.

At the vacuum UV resonance fluorescence port of the detection cell a vacuum monochromator (McPherson, model 218) was used to detect $O(^3P)$ at 130.2 nm and $H(^2S)$ at 121.6 nm with a sensitivity of about 1×10^9 cm^{-3} after excitation by a microwave discharge lamp. Typical reaction parameters were as follows: flow velocity $\bar{v}$, approximately 1200 cm s^{-1}; pressure, about 3 Torr, mainly of helium carrier gas; H_2O_2 concentrations, about (8 - 20) × 10^{12} cm^{-3} in the flow tube and about five times greater in the injector; HO_2 concentration, up to 2×10^{12} cm^{-3}; initial OH concentration, about 4×10^{10} cm^{-3}; detection limit of OH (and, indirectly, of HO_2), in the 10^8 cm^{-3} range.

The apparatus for $N_2(A)$ reaction studies shown in Fig. 2 is similar to that of Fig. 1 in using LIF and vacuum UV resonance fluorescence detection but differs in its range of flow speeds and in the method of reactant generation. Higher flow speeds of 4000 - 5000 cm s^{-1} are required because of the highly efficient wall deactivation of $N_2(A)$. The reaction of argon metastables (produced in a d.c. discharge at 200 V and 1 mA) with N_2 generates moderate concentrations of A state in a carrier gas of about 80% Ar and 20% N_2 at about 1.8 Torr pressure. The other reactant, O_2, is added through a multiperforated glass-loop injector such that mixing is complete within about 2 cm axial distance. Although the injector is movable, it was used at a fixed position 26 cm upstream of the LIF cell, and rate information was obtained by monitoring the decrease in fluorescence signal with increasing O_2 addition at constant reaction time.

$N_2(A)$ was detected by LIF in the first positive system of $N_2(B\ ^3\pi \leftarrow A\ ^3\Sigma_u^+)$ at the P_1 band heads of the $\Delta v = 4$ bands at 618.7, 612.7 and 606.9 nm using a dye-pumped Nd–YAG laser (Chromatix 1000E and 1050). This allowed

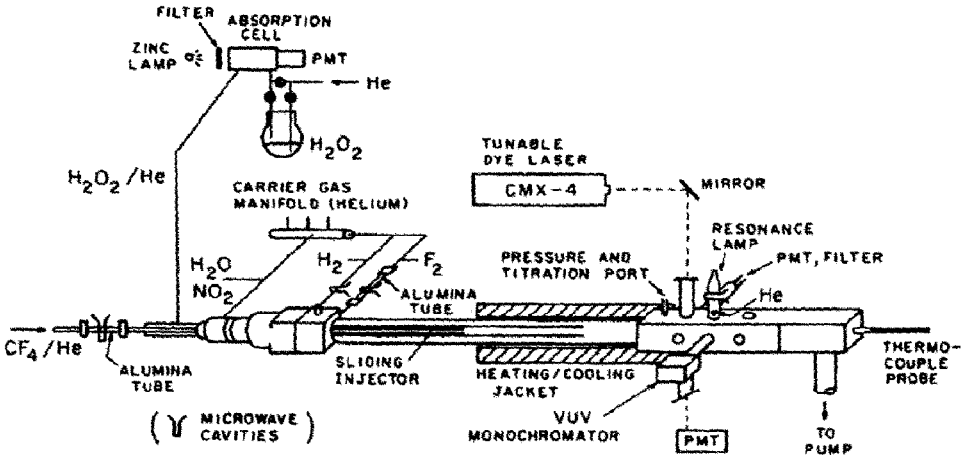

Fig. 1. Diagram of the OH + HO_2 reaction apparatus.

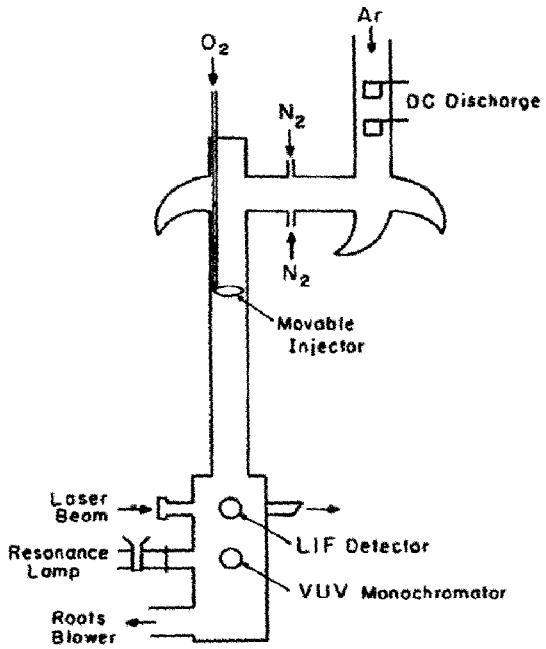

Fig. 2. Diagram of the $N_2(A)$ reaction apparatus.

measurement of the $v = 0$, $v = 1$ and $v = 2$ states and of their specific interaction with O_2. The laser was operated in the burst mode, and the fluorescence signal was collected with a cooled red-sensitive photomultiplier (RCA 31034) gated for 60 μs per laser burst and accumulated for 10 s. The $O(^3P)$ concentra-

tion could be measured 5 cm downstream of the LIF port by vacuum UV resonance fluorescence at 130.2 nm using a vacuum UV monochromator (Jarrell Ash, model 84-110) and a solar-blind photomultiplier (EMR 541GX).

The development of laminar flow and the corresponding transition length were measured using two side-by-side Pitot tubes which mapped the flow radially and axially. The measured pressure differences between the Pitot pointing into the flow and that pointing perpendicular to the flow were corrected for gas compressibility and viscosity and were converted to local flow velocities.

3. Results and discussion

The work on the kinetics of the OH + HO_2 reaction was carried out by Dr. U.C. Sridharan and Mr. L.X. Qiu (Associate Professor on leave from the Institute of Technology of Peking, China). The experiments included extensive absolute calibration of the HO_2 concentration measurement by conversion of HO_2 to OH and comparison with known OH concentrations produced via the H + NO_2 reaction. For a given HO_2 concentration entering the flow tube through the movable injector and mixing with the OH stream generated upstream, the OH concentration was measured by LIF as a function of injector position over a distance of 40 cm in 5 cm intervals. The decay of OH so obtained includes a substantial contribution due to the OH + H_2O_2 reaction [1] which was experimentally determined by repeating the OH concentration *versus* injector position measurements with the CF_4 discharge off. This decay represented only the OH + H_2O_2 reaction, and since only a small fraction of H_2O_2 was converted to HO_2 by reaction with F the difference of the two linear semilogarithmic decay slopes gave the effective first-order rate constant of OH + HO_2 for the particular HO_2 concentration. This subtraction of the two slopes is equivalent to a plot of the log of the ratio of the OH concentrations with the discharge, *i.e.* HO_2, on and off. The injector surface effect which was very small, usually corresponding to a negative slope of less than approximately 2 - 3 s^{-1}, was determined by measuring OH concentration as a function of injector position with only helium addition through the injector. This correction applies to both discharge on and discharge off decays and therefore cancels in the OH + HO_2 rate analysis. Figure 3 shows typical OH decays with and without HO_2, and Fig. 4 shows a plot of the effective first-order rate constant *versus* HO_2 concentration. The good linearity and the absence of a large intercept support the above data analysis. The value of the desired rate constant was found to be (6 - 8) $\times$ 10^{-11} cm^3 s^{-1} in a limited number of early experiments. It is reassuring to note, furthermore, that the measured semilogarithmic [OH] plots with discharge off, corrected slightly for the injector effect, gave values for the rate constant for the OH + H_2O_2 reaction in the range (1.6 - 1.8) $\times$ 10^{-12} cm^3 s^{-1}, in excellent agreement with its accepted value [1, 3]. Further work on the kinetics of this important reaction is in progress, including alternative methods for radical generation and measurement of its temperature dependence.

A brief discussion of its recent history shows large discrepancies that may be partly due to differences in experimental conditions. Several photolysis studies

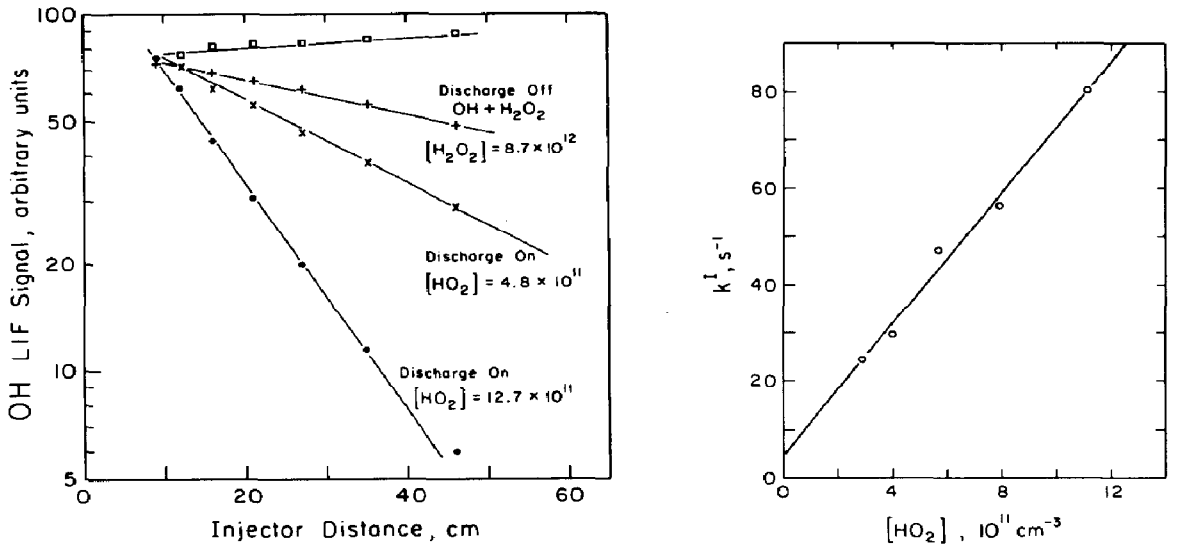

Fig. 3. OH decay plots for reactions with H_2O_2 and with HO_2.

Fig. 4. Plot of the first-order rate constant for OH + HO_2 *vs.* [HO_2].

[4 - 8] have resulted in rate constants of (1 - 2) × 10^{-10} cm^3 s^{-1}, mainly at pressures near 1 atm with H_2O concentrations in the many torrs range, and it has been suggested that the presence and reaction of hydrogen-bonded complexes (*e.g.* $HO_2 \cdot H_2O$) may contribute to the higher values. At lower pressures, in discharge flow systems, the situation is complicated by the fact that some recent researchers [9, 10] have measured rate constant ratios $k(OH + HO_2)/k(OH + H_2O_2)$ but have based their results on an incorrect value of $k(OH + H_2O_2)$, while others [11] have modeled large systems of reactions and have arrived at approximate upper bounds for the desired rate constant. The most recent work [12, 13] at low pressures (approximately 1 - 5 Torr) has favored values of about 6.4×10^{-11} cm^3 s^{-1}. The surprising fact that this reaction is much faster than its two symmetrical counterparts, OH + OH and HO_2 + HO_2, suggests a looser transition state that may, in turn, reflect the much larger exothermicity of the OH + HO_2 reaction (ΔH_{298}° = –69.5 kcal mol^{-1} compared with –16.9 and –27.8 for the other two). Studies of the temperature dependence of all three reactions may clarify the role of long-lived intermediates.

The work on $N_2(A)$ quenching or reaction with O_2 was performed by Mr. M.P. Iannuzzi. The pseudo-first-order reaction (O_2 concentrations were three to four orders of magnitude larger than $N_2(A)$ concentrations) is characterized by linear semilogarithmic plots of the LIF signal I_F due to $N_2(A)$ as a function of the O_2 concentration at constant reaction time t. In the plug flow approximation, the expression for the rate constant k^v for a specific vibrational state (v = 0, 1, 2) is given by $k^v = -t^{-1}\, d(\ln I_F)/d[O_2]$, but because of the partial establishment of laminar flow this must be multiplied by a correction factor α whose value lies between 1 (plug flow) and 1.59 (laminar flow). For the conditions of these experiments, an experimental correction factor of 1.34 arising from

the Pitot tube measurements was used rather than the theoretical value of 1.43 calculated by an approximate solution of the Navier–Stokes equations [14]. Figure 5 shows typical $\ln I_F$ *versus* $[O_2]$ plots for $N_2(A)$, $v = 0, 1, 2$. Repeated measurements gave $k^0 = (2.5 \pm 0.2) \times 10^{-12}$ cm^3 s^{-1}, $k^1 = (3.9 \pm 0.4) \times 10^{-12}$ cm^3 s^{-1} and $k^2 = (4.2 \pm 0.5) \times 10^{-12}$ cm^3 s^{-1}, where the uncertainty is the experimental random error at one standard deviation. When systematic errors due to pressure, flow rates (*i.e.* α) and $d(\ln I_F)/d[O_2]$ slopes are included, the uncertainty is estimated to be about $\pm 15\%$.

Comparison with other recent studies shows good agreement for $v = 0$ and $v = 1$ with Zipf [15] ($k^0 = 1.9$ cm^3 s^{-1}, $k^1 = 4.0 \times 10^{-12}$ cm^3 s^{-1}) and Piper *et al.* [16] ($k^0 = 2.3$ cm^3 s^{-1}, $k^1 = 4.1 \times 10^{-12}$ cm^3 s^{-1}), both of whom used Vegard–Kaplan emission intensities to monitor $N_2(A)$ and were unable to obtain $v = 2$ data. The present work is the first in which LIF was used for such quenching studies and will be expanded to provide data for other quenchers as well as for vibrational relaxation in selected cases. For the O_2 reaction, it is possible from our data to rule out a large contribution due to $v = 1$ to $v = 0$ collisional relaxation, *i.e.* $k^{1\to 0} \lesssim 0.5 \times 10^{-12}$ cm^3 s^{-1}, on the basis of the lack of curvature in the semilogarithmic $N_2(A)$ $v = 0$ plots where extensive cascading would have led to smaller $d(\ln I_F)/d[O_2]$ slopes for low O_2 concentrations.

The interesting question of product channel identity awaits further work, particularly of simultaneous oxygen atom and N_2O yield measurements to verify Zipf's [15] claim that the reactive channels $N_2(A) + O_2(X) \rightarrow N_2O + O(^3P$ or $^1D)$ account for $60\% \pm 20\%$ of the overall process. Aside from N_2O formation, there are exothermic channels to form 2NO in an improbable four-center reaction as well as energy transfer channels to various excited states of O_2 with or

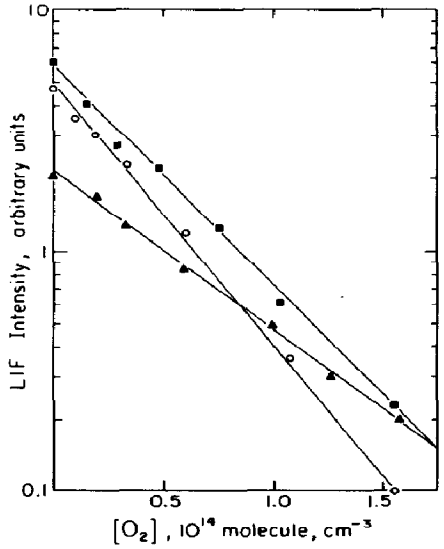

Fig. 5. Typical plots of the $N_2(A)$ LIF signal I_F *vs.* $[O_2]$: ▲, $v = 0, t = 7.19$ ms; ■, $v = 1, t = 6.44$ ms; ○, $v = 2, t = 6.83$ ms.

without subsequent dissociation to $O(^3P)$ depending on whether the energy transferred lies between 5.1 and 6.2 eV or below 5.1 eV.

Lastly, the application of these findings to atmospheric processes should be discussed briefly. The OH + HO_2 reaction is the largest loss process for HO_x above about 30 km in the stratosphere and thereby affects the odd-oxygen budget directly through the HO_x catalytic cycles and indirectly through coupling reactions with NO_x and ClO_x species. The somewhat larger rate constant reported here and in other laboratories ($(6 - 8) \times 10^{-11}$ cm^3 s^{-1} compared with the earlier recommended value of 4×10^{-11} cm^3 s^{-1}) will decrease the calculated model predictions for ozone column reduction due to anthropogenic halocarbon release. The magnitude of this change is now thought to be lower because of increases in rate constants for other reactions that remove HO_x in the lower stratosphere.

The $N_2(A)$ quenching or reaction processes are important in our understanding of auroras but may also have application in questions of the tropospheric N_2O budget.

Low energy electron impact is known to form large amounts of $N_2(A)$ either directly or by radiative cascade from higher triplet states. Cartwright [17] has calculated conversions of about 10^{-6} of all N_2 into $N_2(A)$ at 130 km altitude in an IBC II aurora and about 10^{-8} at 110 km. Above about 120 km, quenching or reaction with $O(^3P)$ is the major loss process, but below 100 km O_2 becomes the most important quencher. This may result in large auroral N_2O source terms, as Zipf and Prasad [18] have proposed. The formation of $N_2(A)$ from nitrogen atoms in lightning arcs may also lead to N_2O production, but this source is probably small compared with biogenic and combustion sources.

Acknowledgments

This work was supported by the National Aeronautics and Space Administration under Grant NGR 39 011 161 and by the Air Force Geophysics Laboratory and Defense Nuclear Agency under Contract F19628-81-K-0022.

References

1 U.C. Sridharan, B. Reimann and F. Kaufman, *J. Chem. Phys., 73* (1980) 1286.
2 C.J. Howard, *J. Am. Chem. Soc., 102* (1980) 6937.
3 L.F. Keyser, *J. Phys. Chem., 84* (1980) 1659.
4 C.J. Hochanadel, J.A. Ghormely and P.J. Ogren, *J. Chem. Phys., 56* (1972) 4426.
5 W.B. DeMore and E. Tschuikow-Roux, *J. Phys. Chem., 78* (1974) 1447.
6 R.R. Lii, R.A. Gorse, Jr., M.C. Sauer and S. Gordon, *J. Phys. Chem., 84* (1980) 819.
7 W.B. DeMore, *J. Phys. Chem., 83* (1979) 1113.
8 C.J. Hochanadel, T.J. Sworski and P.T. Ogren, *J. Phys. Chem., 84* (1980) 3274.
9 W. Hack, A.W. Preuss and H. Gg. Wagner, *Ber. Bunsenges. Phys. Chem., 82* (1978) 1167.
10 J.P. Burrows, D.I. Cliff, G.W. Harris, B.A. Thrush and J.P.T. Wilkinson, *Proc. R. Soc. London, Ser. A, 368* (1979) 463.
11 J.S. Chang and F. Kaufmann, *J. Phys. Chem., 82* (1978) 1683.
12 F. Temps and H. Gg. Wagner, *Bericht 18A/1980* (Max Planck Institut für Strömungsforschung, Göttingen).

13 L.F. Keyser, personal communication.
14 H.L. Langhaar, *Am. Soc. Mech. Eng., Trans., E64* (1942) A55.
15 E.C. Zipf, *Nature (London), 287* (1980) 523.
16 L.G. Piper, G.E. Caledonia and J.P. Kennealy, *J. Chem. Phys., 74* (1981) 2888.
17 D.C. Cartwright, *J. Geophys. Res., 83* (1978) 517.
18 E.C. Zipf and S.S. Prasad, *Nature (London), 287* (1980) 525.